

Balanced gain-loss induces collective dynamics of mechanically coupled resonators in Optomechanics

P. Djorwé,^{1,*} Y. Pennec,^{1,†} and B. Djafari-Rouhani^{1,‡}

¹*Institut d'Electronique, de Microélectronique et Nanotechnologie,
UMR CNRS 8520 Université de Lille, Sciences et technologies, Villeneuve d'Ascq 59652, France*

We investigate collective nonlinear dynamics in a blue-detuned optomechanical cavity that is mechanically coupled to an undriven mechanical resonator. By controlling the strength of the driving field, we engineer a mechanical gain that balances the losses of the undriven resonator. This gain-loss balance corresponds to the threshold where both coupled mechanical resonators enter simultaneously into self-sustained limit cycle oscillations regime. Rich sets of collective dynamics such as in-phase and out-of-phase synchronizations therefore emerge, depending on the mechanical coupling rate, the optically induced mechanical gain and spring effect, and the frequency mismatch between the resonators. Moreover, we introduce the quadratic coupling that induces enhancement of the in-phase synchronization. This work shows how phonon transport can remotely induce synchronization in coupled mechanical resonator array and opens up new avenues for metrology, communication, phonon-processing, and novel memories concepts.

I. INTRODUCTION

Recent progress in nano engineering has led to exotic optomechanical crystals [1],[2], which are able to confine several optical and mechanical modes on a single chip. A lot of attention has been paid to these optomechanical arrays owing to their capabilities to promote new phenomena and applications. These include collective nonlinear dynamics [3], [4], quantum many-body dynamics of photons and phonons [5], long-range coupling of phonon modes [6],[7], photons and phonons transport [8],[9], Anderson localization [10], as well as topological phases of sound and light [11],[12].

Owing to their practical applications in rf communication [13], signal-processing [14], and clock synchronization [15], collective phenomena such as synchronization [16],[17],[18] and frequency locking [19],[20] where recently realized in optomechanical systems. These schemes are different one from another, and each of them having its own specificity. Synchronization of two oscillators in contact and sharing a common optical mode was investigated in [16], while the same configuration was later on extended to multiple resonators in [17]. Another synchronized system, consisting of two spatially separated oscillators integrated in a common optical racetrack cavity was reported in [18]. Besides of these optomechanical synchronizations realizations, frequency locking of two and multiple optomechanical systems were reported respectively in [19] and [20]. In all these works, light is the key element used to couple the optomechanical systems involved. There is a lack of work on optomechanical synchronization where phonons are mediating the coupling between the oscillators. Theoretical investigation of quantum many-body dynamics has been investigated

along this line in [5], where both photons and phonons can hop to nearest neighbor sites, and each optomechanical cell in the array is driven.

In the present work, we propose a blue-detuned optomechanical system that is mechanically coupled to an undriven mechanical resonator. By driving the optomechanical system, we engineer a mechanical gain that will balance the losses of the undriven oscillator. This gain-loss balance threshold induces rich sets of collective nonlinear dynamics in the systems. Our proposal is different of those listed above in at least three points. Indeed, (i) the collective dynamics are induced through mechanical gain-loss balance, (ii) only phonons are mediating the energy transport between the driven and the undriven resonator, and (iii) only one optomechanical cell is excited and the energy is transferred to the rest of the system. By using non-degenerated mechanical resonators, we have identified different sets of synchronized states emerging in our proposal. These synchronized states depend on the mechanical coupling, the mechanical gain, the optical spring effect and the frequency mismatch of the two resonators. Both in-phase and out-of-phase synchronization are present, and the phase transition between these two phenomena happens at a phase flip which has been shown to be related to a high enough value of the mechanical gain. Moreover, we have used the quadratic coupling to enhance in-phase synchronization process. As these rich collective phenomena can be controlled by only tuning the driving field, our proposal appears as a nice platform to perform applications such as phonons transport, phonons processing, and metrology. The rest of the work is organized as follows. In Sec. II, the model and its dynamical equations are described. The emerged collective dynamics are presented in Sec. III, without the quadratic coupling. The frequency mismatch effect together with qualitative explanations of the transitional phases are figured out in Section IV. Section V is devoted to the enhancement effect of the quadratic coupling, while Sec. VI concludes the work.

*Electronic address: philippe.djorwe@univ-lille1.fr

†Electronic address: yan.pennec@univ-lille1.fr

‡Electronic address: bahram.djafari-rouhani@univ-lille1.fr

II. MODELLING AND DYNAMICAL EQUATIONS

Our benchmark system is the one sketched in Fig. 1a, which consists of an optomechanical cavity whose vibrating element is mechanically coupled to an undriven auxiliary mechanical resonator. In the rotating frame of the driving fields (ω_p), the Hamiltonian ($\hbar = 1$) describing this system is,

$$H = H_{OM} + H_{int} + H_{drive}, \quad (1)$$

with

$$\begin{cases} H_{OM} = -\Delta a^\dagger a - g a^\dagger a (b_1^\dagger + b_1) + \sum_{j=1,2} \omega_j b_j^\dagger b_j, \\ H_{int} = -J (b_1 b_2^\dagger + b_1^\dagger b_2), \\ H_{drive} = E (a^\dagger + a). \end{cases} \quad (2)$$

In this Hamiltonian, a and b_j are the annihilation bosonic field operators describing the optical and mechanical resonators, respectively. The mechanical displacements x_j are connected to b_j as $x_j = x_{zPF} (b_j + b_j^\dagger)$, where x_{zPF} is the zero-point fluctuation amplitude of the mechanical resonator. The mechanical frequency of the j^{th} resonator is ω_j and $\Delta = \omega_p - \omega_{cav}$ is the detuning between the optical drive (ω_p) and the cavity frequency (ω_{cav}). The mechanical coupling strength between the two mechanical resonators is J , and the optomechanical coupling is g . The amplitude of the driving pump is E . For large photon number in the system, the quantum operators in Eq. (2) can be treated as complex scalar fields, which are defined as the mean values of the operators: $\langle a \rangle = \alpha$ and $\langle b_j \rangle = \beta_j$. This leads to the following set of classical nonlinear equations for our system,

$$\begin{cases} \dot{\alpha} = [i(\Delta + g(\beta_1^* + \beta_1)) - \frac{\kappa}{2}] \alpha - i\sqrt{\kappa} \alpha^{in}, \\ \dot{\beta}_1 = -(i\omega_1 + \frac{\gamma_1}{2}) \beta_1 + iJ\beta_2 + ig\alpha^* \alpha, \\ \dot{\beta}_2 = -(i\omega_2 + \frac{\gamma_2}{2}) \beta_2 + iJ\beta_1, \end{cases} \quad (3)$$

where optical (κ) and mechanical (γ_j) dissipations have been added, and the amplitude of the driving pump has been substituted as $E = \sqrt{\kappa} \alpha^{in}$ in order to account for losses. In this form, the input laser power P_{in} acts through $\alpha^{in} = \sqrt{\frac{P_{in}}{\hbar\omega_p}}$. Throughout the work, we assume the hierarchy of parameters $\gamma_j, g \ll \kappa \ll \omega_j$, similar to those encountered in resolved sideband experiment [21].

Starting from two non-degenerated mechanical resonators, $\omega_1 \neq \omega_2$ and $\gamma_1 \neq \gamma_2$, we aim to synchronize their motions. Our strategy is based on engineering and control of the mechanical gain, by driving the optomechanical cavity with a blue detuned electromagnetic field. As we increase the driving strength, this generates optical damping (γ_{opt}) that balances the intrinsic damping (γ_1) of the driven mechanical resonator (see green dot in Fig. 1b), which reaches threshold of phonon lasing and starts emitting phonons that are mechanically transferred to the second mechanical resonator (see green dot

in Fig. 1c). This phonon transfer process is revealed through the increase of amplitude of the undriven mechanical resonator as shown in the inset of Fig. 1c. By further increasing the strength of the driving field, the engineered gain increases too and balances the losses of the second mechanical resonator (see magenta dot in Fig. 1b). From this point, the whole system reaches the phonon lasing threshold and both mechanical resonators simultaneously start emitting phonons (see magenta dot in Fig. 1c). After this amplification phase, the system settles into self-sustained mechanical oscillations regime, above which complex nonlinear behaviours such as period doubling and chaos could emerge for strong enough driving strength. As we are looking for collective dynamics such as synchronization and frequency locking phenomena, we limit ourself in this work to the self-sustained oscillations regime. In order to optimize the input power needed to balance gain and losses in the whole system, we require that the first resonator has a higher quality factor than the second one ($\gamma_1 > \gamma_2$). This requirement ensures that our system can reach low-power phonon lasing, which is a useful prerequisite for experimental test of our proposal.

III. COLLECTIVE DYNAMICAL STATES

Beyond the phonon lasing threshold, both mechanical resonators exhibit limit cycle oscillations, which are correlated through their phases and/or their vibrational amplitudes. These correlations lead to different sets of collective nonlinear behaviours, ranging from in-phase to out-of-phase synchronizations with equal or mismatched amplitudes. We have characterized these behaviours from steady state solutions of the mechanical resonators, where all the transient behaviour has died out. The overall dynamics is shown in Fig. 1d. The blue area is the linear regime, which is characterized by fixed points and where there is an energy flow from the driven resonator (β_1) into the undriven one (β_2) as depicted in the inset of Fig. 1c. At the gain and loss balance, the parametric instability threshold is reached, and phonon amplification process happens (gray area) until the mechanical amplitudes settle into the self-sustained oscillations regime due to the intrinsic nonlinearity in the system. Therefore, depending on the strength of both mechanical coupling J and driving field α^{in} , the resonators display several sets of collective dynamical state as shown by different colors beyond the gray area in Fig. 1d. Two quantities have been defined to characterize these dynamical states, the phase difference between the resonators and their mismatched amplitudes that is termed error synchronization later on. The instantaneous phase ϕ of a given resonator is defined as, $\phi = \text{atan} \left(\frac{\text{Im}(\beta)}{\text{Re}(\beta)} \right)$, where β is a mechanical state variable. The averaged phase difference ($\Delta\phi$) between both resonator is,

$$\Delta\phi = \langle |\phi_i - \phi_j| \rangle \quad i, j = 1, 2 \quad (4)$$

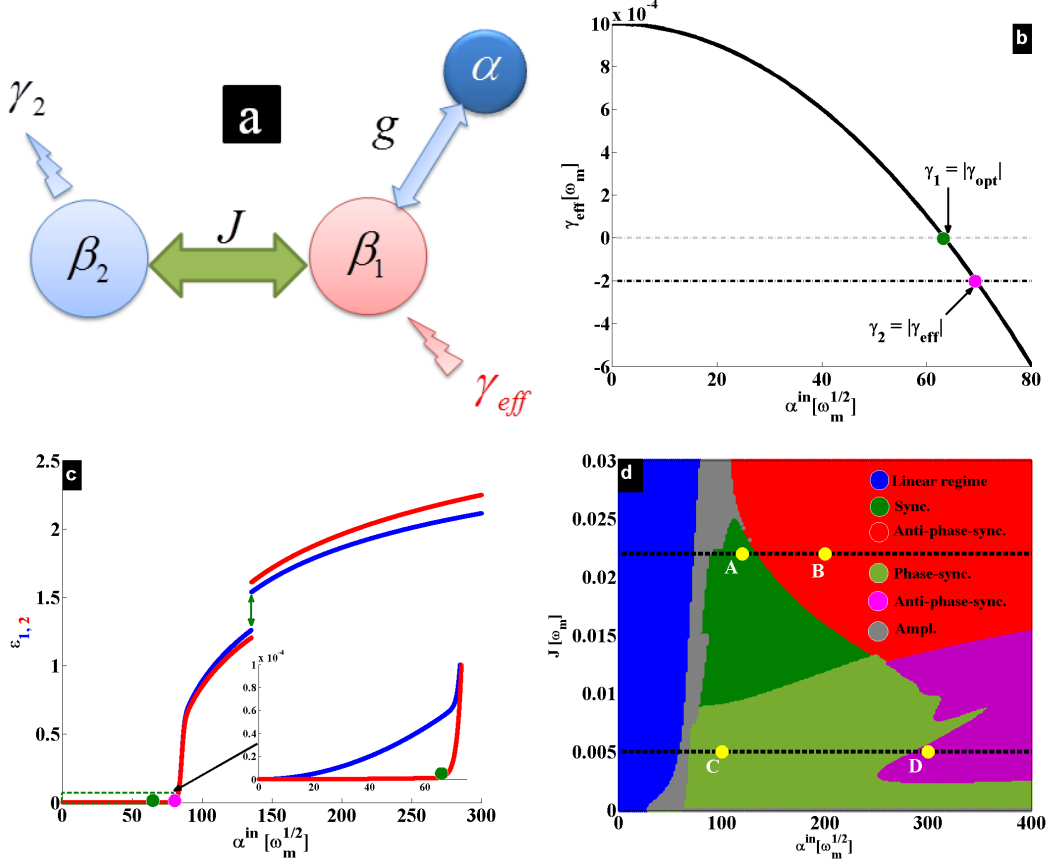


FIG. 1: (a) Benchmark system consisting of a blue-detuned driven optomechanical cavity, which is mechanically coupled to an undriven mechanical resonator. (b) Diagram displaying collective dynamics in the (α^{in}, J) parameter's space. Once the losses are balanced by the gain, both mechanical resonators carry out different type of dynamics depending on the values of α^{in} and J . The used parameters are, $\omega_1 = \omega_m$, $\omega_2 = 1.002\omega_m$, $\gamma_1 = 10^{-3}\omega_m$, $\gamma_2 = \frac{\gamma_1}{5}$, $\kappa = 10^{-1}\omega_m$, $g = 2.5 \times 10^{-4}\omega_m$, $\Delta = \omega_m$.

where $\langle \cdot \rangle$ denotes an average over time. Similarly, the steady state amplitude of a given resonator is captured by $\epsilon \equiv \text{rms}(\beta)$, where “rms” is the root-mean-square value. We define the synchronization error here as a difference between the amplitudes of the resonators,

$$\text{Err} = |\epsilon_i - \epsilon_j| \quad i, j = 1, 2. \quad (5)$$

Depending on these two quantities, the system exhibits four different dynamical states as depicted beyond the gray area in Fig. 1b. In the green area, one has both $\Delta\phi \sim 0$ and $\text{Err} \sim 0$, resulting in a synchronized state of the mechanical resonators as dynamically depicted in Fig. 2a. It can be clearly seen that both resonators exhibit a similar behaviour in this regime. In the light green area, both resonators are still in phase ($\Delta\phi \sim 0$), but they have different amplitudes $\text{Err} \neq 0$. Therefore, complete synchronization is missing, and the resonators carry out phase synchronization as dynamically shown in Fig. 2b. Similar dynamical structure exists also when the resonators are out of phase ($\Delta\phi \sim \pi$). Indeed, anti-synchronization is achieved in the red area ($\text{Err} \sim 0$), where the resonators oscillate with identical amplitudes

but are out of phase. Such a dynamic is depicted in Fig. 2c, which reveals π -synchronization of both mechanical resonators over time. Moreover, the resonators exhibit an anti-phase synchronization in the magenta area, where they evolve out of phase from each other with dissimilar vibrational amplitudes ($\text{Err} \neq 0$) as it can be seen in Fig. 2d. These sets of dynamical states enabled by our proposal reveal its performance in carrying out rich collective dynamics compared to those known in the state of art optomechanical systems. The key point of this performance here is the presence of gain and loss, which induces the different phase transitions observed in Fig. 1d as we will explain later on. From these displayed collective dynamics, one can deduce two features depending on either the mechanical coupling J or the driven strength α^{in} is adjusted. For weak mechanical coupling for instance, the two mechanical resonators start exhibiting phase synchronization, which ends up to complete synchronization as J is increasing. This is the case for the transition from the light green to the green areas in Fig. 1d. Similar transition happens when the resonators are out of phase as well, where the increase of J

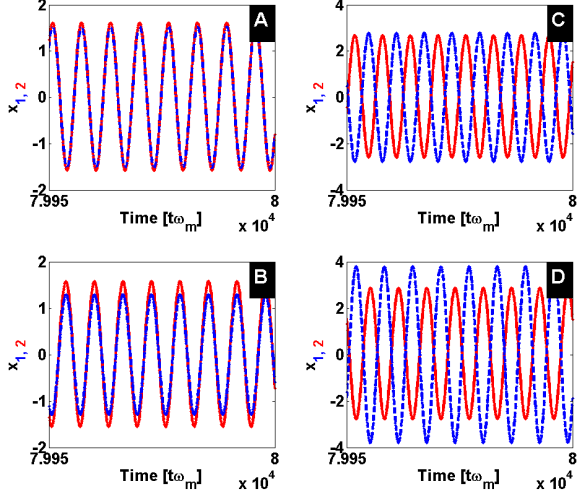


FIG. 2: (a), (c) 0, π -synchronization states. (b), (d) Phase, anti phase synchronizations. In (a) and (c), $J = 2.2 \times 10^{-2} \omega_m$ and $\alpha^{in} = (1.2 \times 10^2, 2.2 \times 10^2) \sqrt{\omega_m}$, respectively. In (b) and (d), $J = 5 \times 10^{-3} \omega_m$ and $\alpha^{in} = (10^2, 3 \times 10^2) \sqrt{\omega_m}$, respectively.

adjusts their vibrational amplitudes (see switching from magenta to red areas in Fig. 1d). One can point out also the fact that, the driving strength mostly induces switching related to the phase of the resonators. Indeed, as α^{in} is increasing, the resonators switch from being in phase ($\Delta\phi \sim 0$) to completely be out of phase ($\Delta\phi \sim \pi$). This feature can be seen for instance from the transitions between the green and the red areas in Fig. 1d. This switching that is termed later on as phase-flip, is a well-known nonlinear phenomenon characterized by a sudden jump of the phase difference roughly from 0 to π [22],[23]. We have figured out this phenomenon in Fig. 3, where the phase difference given in Eq. (4) (see dashed line gray color) and the synchronization error defined in Eq. (5) (see full line black color) are represented for a given $J = 2.2 \times 10^{-2} \omega_m$. It can be clearly seen that after the amplification regime, both mechanical resonators adjust their amplitude and phase, and synchronize for a while within the range $(100 \leq \alpha^{in} \leq 135) \sqrt{\omega_m}$. Beyond the upper limit of this interval, the phase difference suddenly jumps from roughly 0 to π while the synchronization error remains almost zero ($\text{Err} \sim 0$). This phase-flip phenomenon marks the threshold of the out of phase synchronization, which is induced both by gain-loss competition and optical spring effect through an adjustment of the driving strength. We have found that the phase-flip transition is likewise revealed through the amplitude jump phenomenon, pointed out by the green double arrow indicated in Fig. 1c. This can be qualitatively explained by an analytical approach based on the mechanical eigenmodes of our system.

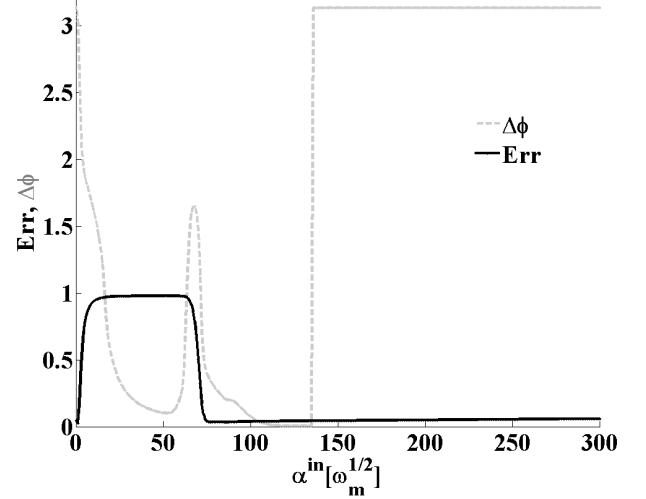


FIG. 3: Phase difference $\Delta\phi$ (dashed gray color) and error synchronization Err (full dark color) between the mechanical resonators for $J = 2.2 \times 10^{-2} \omega_m$.

IV. ANALYTICAL APPROXIMATIONS AND FREQUENCY MISMATCH EFFECT

Based on well-known analytical approximations [24], the mechanical eigenmodes of our system can be obtained by integrating the optical intracavity field $\alpha(t)$ out of the set of Eq. (3). The resulting eigenmodes yield,

$$\lambda_{\pm} = \frac{\omega_{\text{eff}} + \omega_2}{2} - \frac{i}{4} (\gamma_{\text{eff}} + \gamma_2) \pm \frac{\sigma}{4}, \quad (6)$$

where $\omega_{\text{eff}} = \omega_1 + \delta\omega_{\text{opt}}$ and $\gamma_{\text{eff}} = \gamma_1 + \gamma_{\text{opt}}$ are the effective frequency and damping of the driven mechanical resonator, respectively. The quantities $\delta\omega_{\text{opt}}$ and γ_{opt} are respectively the optical spring effect and damping induced by the driving field [24]. The phonon lasing threshold and the phase flip phenomena can be explained through the complex quantity σ whose real and imaginary parts are given by,

$$\text{Re}(\sigma) = \sqrt{\frac{\chi^2 + (4\Delta\omega_{\text{eff}}\Delta\gamma_{\text{eff}})^2 + \chi}{2}}, \quad (7)$$

and

$$\text{Im}(\sigma) = \sqrt{\frac{\chi^2 + (4\Delta\omega_{\text{eff}}\Delta\gamma_{\text{eff}})^2 - \chi}{2}}, \quad (8)$$

where $\chi = 16J^2 + 4\Delta\omega_{\text{eff}}^2 - \Delta\gamma_{\text{eff}}^2$ with $\Delta\omega_{\text{eff}} = \omega_{\text{eff}} - \omega_2$ and $\Delta\gamma_{\text{eff}} = \gamma_2 - \gamma_{\text{eff}}$. From Eqs.(6)-(8), it appears that the mechanical supermodes are generally characterized by the frequencies ($\text{Re}(\lambda_{\pm}) = \omega_{\pm}$) and dampings ($\text{Im}(\lambda_{\pm}) = \gamma_{\pm}$) given by,

$$\omega_{\pm} = \frac{\omega_{\text{eff}} + \omega_2}{2} \pm \frac{\text{Re}(\sigma)}{4}, \quad (9)$$

and

$$\gamma_{\pm} = -\frac{(\gamma_{\text{eff}} + \gamma_2)}{4} \pm \frac{\text{Im}(\sigma)}{4}. \quad (10)$$

These general expressions of frequencies and dissipations of the supermodes given in Eqs.(9)-(10) reveal the dissipative Rabi oscillations that arise in the system. Such dynamics are carried out in the linear regime (blue area in Fig. 1d). However, owing to the driving that induces control of both the mechanical gain (γ_{opt}) and optical spring effect ($\delta\omega_{\text{opt}}$), specific cases of Eqs.(9)-(10) can be derived. For degenerated mechanical resonators for instance ($\omega_1 = \omega_2$), one gets $\Delta\omega_{\text{eff}} \sim 0$ for a weak driving field. At the balanced gain and loss, it results that $\text{Im}(\sigma) = 0$ and $\text{Re}(\sigma) = \sqrt{16J^2 - \Delta\gamma_{\text{eff}}^2}$. This leads to a well-known exceptional point (EP) at $J = \frac{\Delta\gamma_{\text{eff}}}{4}$ [25], where Rabi oscillations cease, and this marks the threshold of phonon lasing where the mechanical resonators exhibit self-sustained limit cycle oscillations. In our proposal however, there is a frequency mismatch $\delta\omega = \omega_2 - \omega_1$, which acts as a perturbation on the EP feature. Interestingly, the phonon amplification process is robust enough against the effect of this mismatch such that, phonon lasing phenomenon still happens at the vicinity of this perturbed EP. Indeed, the mechanical gain can be made enough to overcome the perturbation induced by $\delta\omega$. This happens closer to the balanced gain-loss and for $\chi = 0$, which leads to $\text{Re}(\sigma) = \text{Im}(\sigma) = \sqrt{2\Delta\omega_{\text{eff}}\Delta\gamma_{\text{eff}}}$. Therefore, both mechanical supermodes are amplified at first for a while, and soon after they start dissipating differently through $\sim \pm\sqrt{\frac{\Delta\omega_{\text{eff}}\Delta\gamma_{\text{eff}}}{8}}$. It follows that one of the supermodes is amplified, while the other one will decay until its extinction. At this stage, the motions of the mechanical resonators, which are fully captured through their amplified supermodes (ω_+, γ_+), exhibit in-phase synchronization (Appendix A). As the increase of the driving field is further enhancing the gain, the optical spring effect increases as well, and become comparable to the mismatch leading to $\Delta\omega_{\text{eff}} = \omega_{\text{eff}} - \omega_2 = \delta\omega_{\text{opt}} - \delta\omega \sim 0$. The gain reach likewise high value that is enough to reverse the sign of χ , which becomes negative ($16J^2 + 4\Delta\omega_{\text{eff}}^2 < \Delta\gamma_{\text{eff}}^2$). Using the conditions $\chi < 0$ and $\delta\omega_{\text{opt}} \sim \delta\omega$ in Eqs.(7)-(8) lead to $\text{Re}(\sigma) = 0$ and $\text{Im}(\sigma) = \sqrt{\chi_0}$, where $\chi_0 = \Delta\gamma_{\text{eff}}^2 - 16J^2$. It results that σ is a purely imaginary quantity, and this reversal process is responsible of phase flip in our system. Moreover, $\text{Re}(\sigma) = 0$ means that one supermode has vanished (ω_-, γ_-), which is reminiscent of the amplitude death phenomenon that is a well-known process behind phase flip transition [22],[23]. From the above discussion, it follows that both mechanical gain and optical spring are the key points for the collective phenomena arising in our context. Owing to the

fact that these quantities are tuned through the driving field, our proposal appears as a nice platform to generate collective phenomena, where the system is wholly controlled externally. From the above qualitative expla-

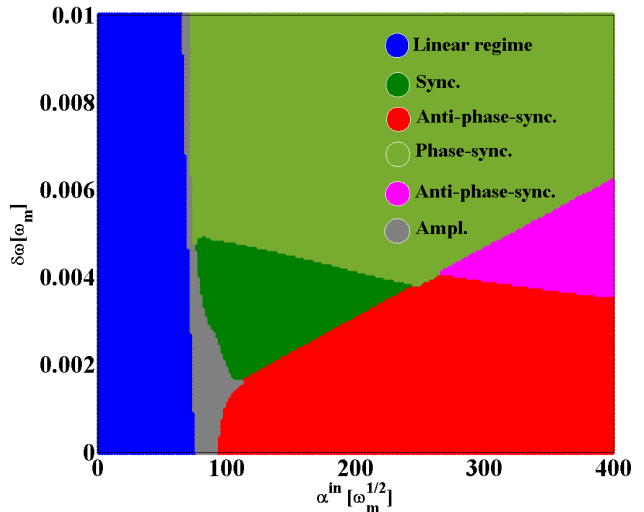


FIG. 4: Numerical diagram displaying collective dynamics in the $(\alpha^{\text{in}}, \delta\omega)$ parameter's space for $J = 2.2 \times 10^{-2}\omega_m$. The other parameters are as in Fig. 1.

nations based on the mechanical eigenmodes, it follows obviously that frequency mismatch is an important parameter, so that a particular attention must be paid on it. Therefore, the effect of $\delta\omega$ on the organization of the collective dynamics is shown in Fig. 4, for a fixed coupling strength $J = 2.2 \times 10^{-2}\omega_m$. It can be seen that, the frequency mismatch very weakly shifts the lasing threshold (transition between blue and gray areas), compared to the coupling strength J (as in Fig. 1d). This feature simply reveals the robustness of the amplification process at the vicinity of the EP, against moderate frequency mismatches as aforementioned. From Fig. 4, this robustness is roughly preserved up to 1% of frequency mismatch. However, just above the lasing threshold, the mismatch induces new reorganization of collective dynamics. For a weak mismatch ($\delta\omega < 2 \times 10^{-3}\omega_m$), π -synchronization is the dominant dynamics. This is expected and is explained by the fact that, weak driving strength is required for the mechanical gain and optical spring effect to reverse the sign of χ and to compensate the mismatch, respectively. For large mismatch however, strong driving strength is required to generate large gain and optical spring effect. Therefore, it is hard to reach π -synchronization in such a configuration as it can be seen for $\delta\omega \gtrsim 5 \times 10^{-3}\omega_m$, where only phase synchronization emerges. For intermediate values of the mismatch ($2 \times 10^{-3}\omega_m \lesssim \delta\omega \lesssim 4 \times 10^{-3}\omega_m$), both resonators can synchronize for a while before switching to out of phase synchronization. Owing to the difficulties of engineering identical mechanical resonators in micro/nano-

fabrication technologies, it could be interesting to seek an enhancement strategy of the observed collective phenomena.

V. QUADRATIC COUPLING ENHANCES IN-PHASE DYNAMICS

In order to assist the role played by the optical spring effect and to enhance effect of the mechanical gain, we have introduced the quadratic coupling (g_{ck}) in the system. This well-known nonlinearity can be generated by inserting the driven mechanical resonator inside the optical cavity instead. The resulted system can be thought as a membrane-in-the-middle setup where the moving element is mechanically coupled to the undriven mechanical resonator. In such a system, the frequency of the driven mechanical system yields $\bar{\omega}_1 = \omega_1 - g_{ck}\alpha^*\alpha$, which can be tuned through the driving field (see Appendix B). This frequency control is useful to bring closer the frequencies of the non-degenerated mechanical resonators involved in our system, even at the vicinity an EP [25]. This can be seen by comparing Fig. 5a to Fig. 3. Indeed, phase synchronization ($\Delta\phi = 0$) is established before $\alpha^{in} = 10^2\sqrt{\omega_m}$ in Fig. 5a where the quadratic term is $g_{ck}/g = -10^{-3}$, whereas this happens above such a value in Fig. 3a where $g_{ck}/g = 0$. It can be also seen that phase synchronization is wider in Fig. 5a than in Fig. 3, revealing the effect of the quadratic coupling in enhancing in-phase synchronization. This enhancement effect of the quadratic term is depicted in Fig. 5b, where in-phase synchronization (green area) is clearly improved. Moreover, by comparing the diagrams depicted in Fig. 5b and Fig. 1d, it results that quadratic coupling also reorganizes localization of the different dynamical states. We have checked the dynamics for the labeled points in Fig. 5b, and the corresponding dynamical states satisfy the expected behaviours. Furthermore, the dynamical state of the gray area intertwined in the magenta zone as been figured out, and its corresponds to a strong coupling regime where both resonators exchange energy through Rabi oscillations (Appendix B).

VI. CONCLUSION

We have investigated collective dynamics in a blue-detuned optomechanical cavity that is mechanically coupled to an undriven mechanical resonator. When the optomechanically engineered mechanical gain balances the losses of the undriven resonator, phonon lasing threshold happens and both resonators simultaneously exhibit self-sustained limit cycles, leading to interesting sets of collective dynamics. Depending on the mechanical coupling and the external driving field, we have observed in-phase and out-of-phase synchronizations that mainly result from process of driving that induces both mechanical gain and optical spring. Qualitative explana-

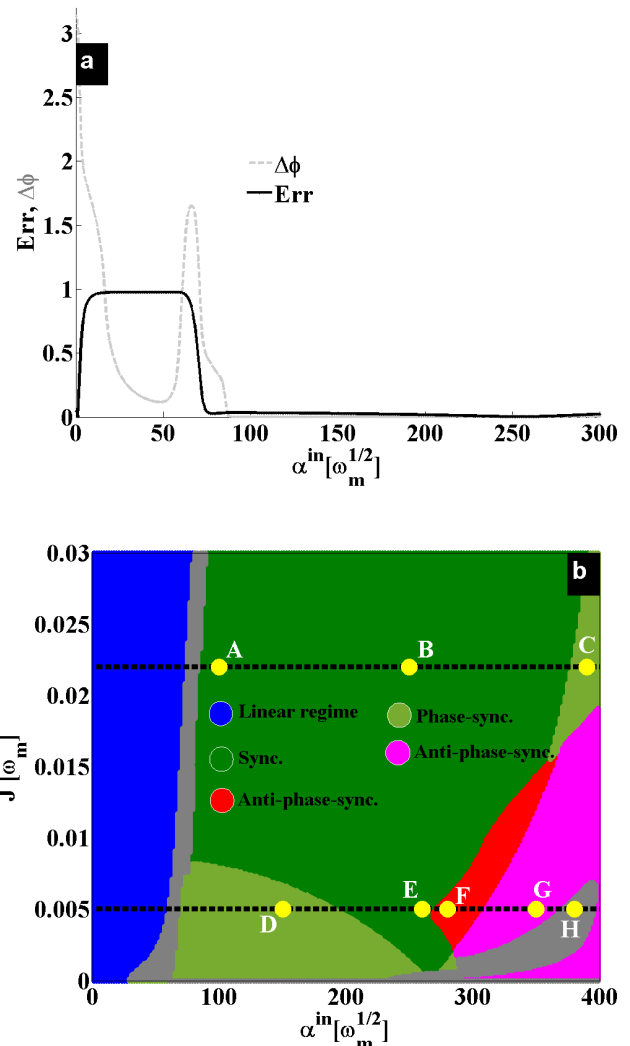


FIG. 5: Enhancement effect of the quadratic coupling on in-phase synchronization. (a) Phase difference $\Delta\phi$ (dashed gray color) and error synchronization Err (full dark color) between the mechanical resonators for $J = 2.2 \times 10^{-2}\omega_m$. (b) Numerical diagram displaying collective dynamics in the (α^{in}, J) parameter's space. Quadratic coupling of $g_{ck}/g = -10^{-3}$ has been accounted, and the others parameters are the same as in Fig. 1.

tions of the main phase transitions arising in our proposal have been provided, based on mechanical eigenvalues evaluated through analytical approximations. Furthermore, we have used quadratic optomechanical coupling to enhance in-phase synchronization between the non-degenerated mechanical resonators involved in the system. Our work opens new avenues towards collective dynamics in an array of mechanically coupled resonators by only driving one of them. This scheme can be extended to related systems including, electromechanical and superconducting microwave setups.

Acknowledgments

This work was supported by the European Commission FET OPEN H2020 project PHENOMEN-Grant Agreement No. 713450.

Appendix A: Mechanical supermodes

In order to show the kind of amplitude death phenomenon that arises in our system, we have numerically extracted the vibrational amplitudes of the supermodes $(\omega_{\pm}, \gamma_{\pm})$. These amplitudes (ε_{\pm}) , which correspond to the frequencies ω_{\pm} , are obtained from the fast Fourier transform (FFT) of the steady states of Eq.(3). We have shown these amplitudes in Fig. 6, where similarities can be seen with Fig. 1c. However, the amplified (ω_{+}, γ_{+}) and dissipated (ω_{-}, γ_{-}) modes are distinguished in Fig. 6 (see green box). Moreover, it can be seen that the amplitude of the dissipated mode (ε_{-}) is not yet negligible at the vicinity of $\alpha^{in} = 10^2 \sqrt{\omega_m}$, which precludes any synchronization in the system (see also Fig. 3). Thereafter, ε_{-} becomes negligible and the motions of the mechanical resonators synchronize on ε_{+} , which mainly captures their amplitudes. By further increasing the driving strength, the amplitude ε_{-} vanishes and this induces amplitude jump phenomenon that happens exactly at the phase-flip transition (see green double arrow and compare it with Fig. 1c).

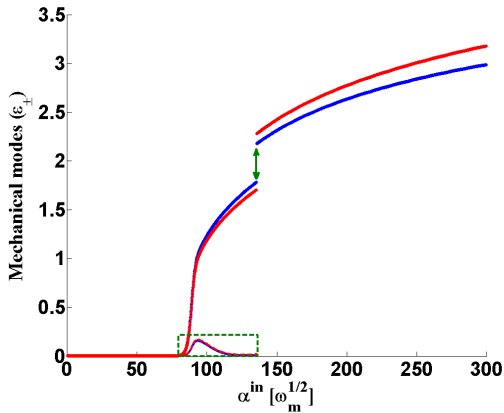


FIG. 6: (a) Mechanical supermodes amplitudes (ε_{\pm}) versus α^{in} at $J = 2.2 \times 10^{-2} \omega_m$, where both amplitude death and jump phenomenon are highlighted. The others parameters are the same as in Fig. 1.

Appendix B: Quadratic coupling and dynamical states

By taking into account the quadratic coupling (or cross-Kerr) in the model, the Hamiltonian becomes,

$$H = H_{OM,ck} + H_{int} + H_{drive}, \quad (B1)$$

with

$$\begin{cases} H_{OM,ck} = -\Delta a^\dagger a + \sum_{j=1,2} \omega_j b_j^\dagger b_j \\ -g a^\dagger a (b_1^\dagger + b_1) - g_{ck} a^\dagger a b^\dagger b, \\ H_{int} = -J(b_1 b_2^\dagger + b_1^\dagger b_2), \\ H_{drive} = E(a^\dagger + a), \end{cases} \quad (B2)$$

where ck stands for “cross-Kerr” and accounts for the quadratic coupling. This leads to the following classical set of nonlinear equations,

$$\begin{cases} \dot{\alpha} = [i(\Delta + g(\beta_1^* + \beta_1) + g_{ck}\beta_1^*\beta_1) - \frac{\kappa}{2}] \alpha - i\sqrt{\kappa} \alpha^{in}, \\ \dot{\beta}_1 = -(i\tilde{\omega}_1 + \frac{\gamma_1}{2}) \beta_1 + iJ\beta_2 + ig\alpha^* \alpha, \\ \dot{\beta}_2 = -(i\omega_2 + \frac{\gamma_2}{2}) \beta_2 + iJ\beta_1, \end{cases} \quad (B3)$$

where $\tilde{\omega}_1 = \omega_1 - g_{ck}\alpha^* \alpha$ is the optically tunable mechanical frequency mentioned in the main text.

The cross-Kerr effect has been pointed out in the main text through Fig. 5, and it has been shown that it enhances in-phase synchronization. This enhancement is related to the control of the frequency mismatch through $\tilde{\omega}_1 = \omega_1 - g_{ck}\alpha^* \alpha$. As we have the frequency hierarchy of $\omega_1 < \omega_2$, we have conveniently used a negative quadratic term ($g_{ck} < 0$) in order to minimize the effect of $\delta\omega$. The dynamical states of the points labeled in Fig. 5b are shown in Fig. 7. It can be clearly seen that these dynamics agree well with the collective behaviours displayed in Fig. 5b. Furthermore, the dynamical state carried out in the gray area intertwined in the magenta zone in Fig. 5b is revealed. It results that, the mechanical resonators exhibit Rabi oscillations within this regime, which means that they are strongly coupled and can exchange energy.

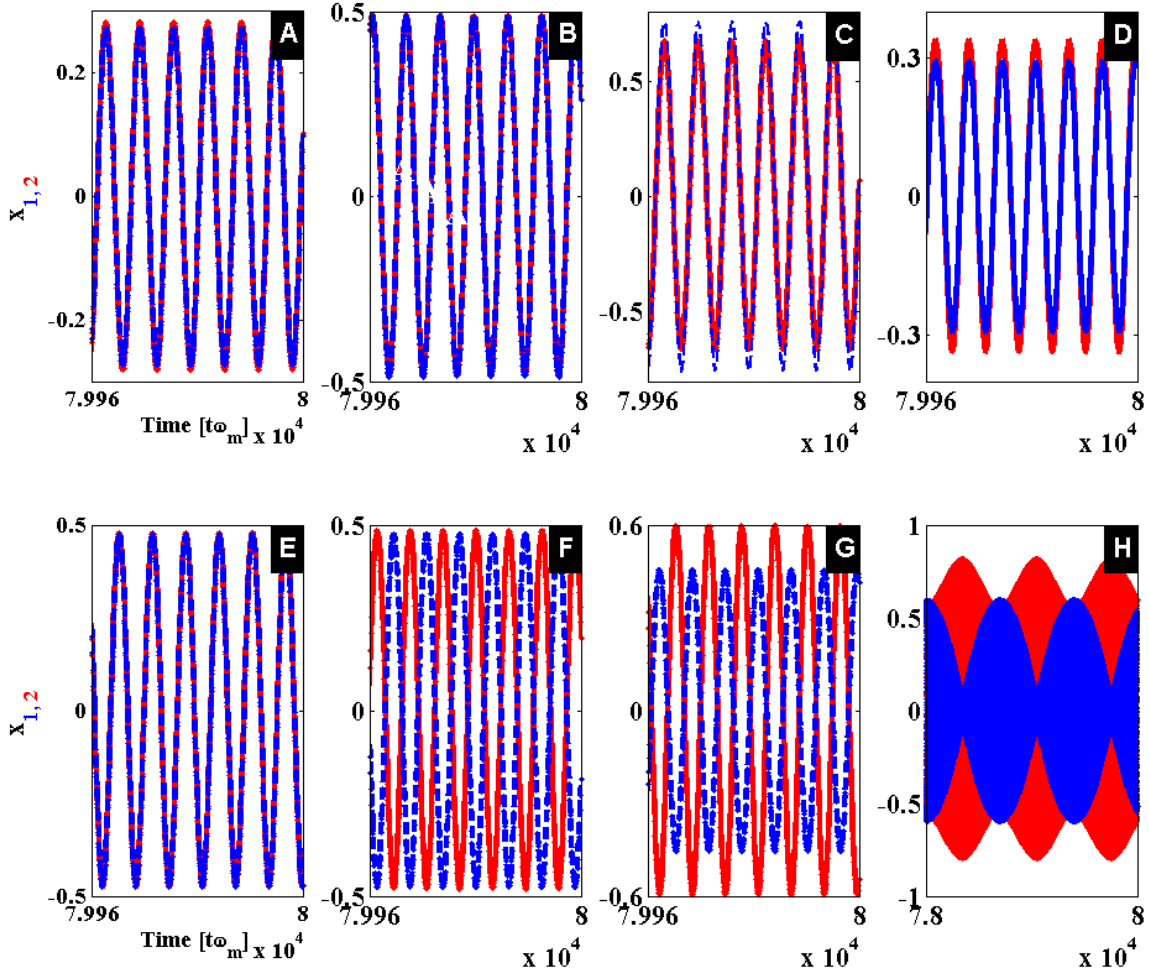


FIG. 7: Dynamical states of the points labeled in Fig. 5b.

-
- [1] M. Eichenfield, J. Chan, R. M. Camacho, K. J. Vahala, O. Painter, Optomechanical crystals, *Nature* **462**, 78–82 (2009); *Ibis*, *Nature* **459**, 550–555 (2009).
- [2] D. E. Chang *et al.*, Slowing and stopping light using an optomechanical crystal array, *New J. Phys.* **13**, 023003 (2011).
- [3] G. Heinrich *et al.*, Collective Dynamics in Optomechanical Arrays, *Phys. Rev. Lett.* **107**, 043603 (2011).
- [4] C. B. Wallin *et al.*, Nondegenerate Parametric Resonance in Large Ensembles of Coupled Micromechanical Cantilevers with Varying Natural Frequencies, *Phys. Rev. Lett.* **121**, 264301 (2018).
- [5] M. Ludwig, and F. Marquardt, Quantum Many-Body Dynamics in Optomechanical Arrays, *Phys. Rev. Lett.* **111**, 073603 (2013).
- [6] A. Xuereb, C. Genes, and A. Dantan, Strong Coupling and Long-Range Collective Interactions in Optomechanical Arrays, *Phys. Rev. Lett.* **109**, 223601 (2012).
- [7] A. Xuereb, C. Genes, G. Pupillo, M. Paternostro, and A. Dantan, Reconfigurable Long-Range Phonon Dynamics in Optomechanical Arrays, *Phys. Rev. Lett.* **112**, 133604 (2014).
- [8] W. Chen, and A. A. Clerk, Photon propagation in a one-dimensional optomechanical lattice, *Phys. Rev. A* **89**, 033854 (2014).
- [9] M. Schmidt, V. Peano, and F. Marquardt, Optomechanical Dirac physics, *New J. Phys.* **17**, 023025 (2015).
- [10] T. F. Roque, V. Peano, O. M. Yevtushenko, and F. Marquardt, Anderson localization of composite excitations in disordered optomechanical arrays, *New J. Phys.* **19**, 013006 (2017).
- [11] V. Peano, C. Brendel, M. Schmidt, and F. Marquardt, Topological Phases of Sound and Light, *Phys. Rev. X* **5**, 031011 (2015).

- [12] C. Brendel, V. Peano, O. Painter, F. Marquardt, Snowflake phononic topological insulator at the nanoscale, *Phys. Rev. B* **97**, 020102(R) (2018).
- [13] S. Bregni, *Synchronization of Digital Telecommunications Networks* (John Wiley, New York, 2002).
- [14] S. Strogatz, *Sync: The Emerging Science of Spontaneous Order* (Hachette Books, New York, 2003).
- [15] T. B. Bahder, *Clock Synchronization and Navigation in the Vicinity of the Earth* (Nova Science, Hauppauge, 2009).
- [16] M. Zhang, G. S. Wiederhecker, S. Manipatruni, A. Barnard, P. McEuen, and M. Lipson, *Phys. Rev. Lett.* **109**, 233906 (2012).
- [17] M. Zhang, S. Shah, J. Cardenas, and M. Lipson, *Phys. Rev. Lett.* **115**, 163902 (2015).
- [18] M. Bagheri, M. Poot, L. Fan, F. Marquardt, and H. X. Tang, *Phys. Rev. Lett.* **111**, 213902 (2013).
- [19] S. Y. Shah, M. Zhang, R. Rand, and M. Lipson, *Phys. Rev. Lett.* **114**, 113602 (2015).
- [20] E. Gil-Santos et al., *Phys. Rev. Lett.* **118**, 063605 (2017).
- [21] S. Hong et al., Hanbury Brown and Twiss interferometry of single phonons from an optomechanical resonator, *Science* **358**, 203 (2017).
- [22] R. Karnatak et al., Nature of the phase-flip transition in the synchronized approach to amplitude death, *Phys. Rev. E* **82**, 046219 (2010).
- [23] A. Sharma et al., Phase-flip transition in nonlinear oscillators coupled by dynamic environment, *Chaos* **22**, 023147 (2012).
- [24] P. Djourwe, Y. Pennec, and B. Djafari-Rouhani, Frequency locking and controllable chaos through exceptional points in optomechanics, *Phys. Rev. E* **98**, 032201 (2018).
- [25] P. Djourwe, Y. Pennec, and B. Djafari-Rouhani, Exceptional point enhances sensitivity of optomechanical mass sensors, arXiv:1903.02542.